Published in: Thin solid films (1997), vol. 310, iss. 1-2, pp. 148-155
Status: Postprint (Author's version)

Characterization of polyacrylonitrile films grafted onto nickel by ellipsometry, atomic force microscopy and X-ray reflectivity

C. Calberg (1), M. Mertens (1) , R. Jérôme (1), X. Arys (2),A.M. Jonas (2), R. Legras (2)

(1) Center for Education and Research on Macromolecules (CERM), University of Liège, Sart Tilman, B-4000Liège, Belgium
(2) Unité de Physique et de Chimie des Hauts Polymères, Université Catholique de Louvain, Place Croix du Sud 1, B-1348 Louvain-la-Neuve, Belgium

Abstract

The thickness and roughness of polyacrylonitrile films electrografted on a nickel surface have been measured by ellipsometry, atomic force microscopy and X-ray reflectivity. From combined ellipsometry and X-ray reflectivity measurements, accurate values for the refractive indices of polyacrylonitrite and nickel have been derived at a 6328-A wavelength. Dependence of the film thickness on the monomer concentration has been quantified for the first time. Furthermore, the thickness of the polyacrylonitrile (PAN) film is related to the nature of the solvent, depending on whether it is a good solvent for PAN (dimethylformamide; DMF) or not (acetonitrile; ACN).

Keywords: Electrochemistry; Ellipsometry; Nickel; Polymers

1. Introduction

The surface properties of metals are currently modified by organic coatings in order to comply with requirements for various industrial applications. The organic film is commonly deposited by either electropolymerization or sputtering. The main limitation of this general strategy is the poor adhesion of the organic layer to the substrate, or at least its poor ageing resistance. The grafting, i.e., the chemical bonding, of the polymer to the metal would be by far the best way of alleviating this disappointing situation. In this respect, the report by Lecayon et ai. [1] that acrylonitrile (AN) can be electrografted onto usual metals, such as nickel and iron, in acetonitrile (ACN) added with tetraethylammonium perchlorate (TEAP: 0.05 M) was a breakthrough. We have recently confirmed the feasibility of the cathodic AN etectrografting and reported that only the first (less cathodic) of the two peaks observed by voltammetry leads to the grafting reaction according to a free radicat mechanism [2]. The inhibition of the electrode as a result of the polymer grafting is clearly observed by voltammetry (Fig. 1) and is the signature for this unusual chimisorption. The intensity of the inhibition peak has also been observed to depend on the monomer concentration. It might thus be anticipated that the thickness of the PAN film grafted at a constant potential in the range of the inhibition peak would also depend on that experimental parameter. Since it might be desirable to control the film thickness and roughness depending on the envisioned applications, we have undertaken a study of these characteristics as a function of solvent and AN concentration, using X-ray reflectivity (XRR), ellipsometry, and atomic force microscopy (AFM) as characterization tools.

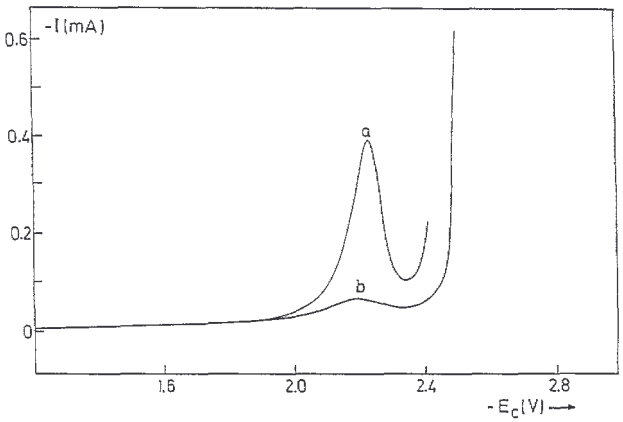

Fig. 1. Comparison of the first (a) and the second (b) potential scan on the same Ni cathode in a 0.05-M TEAP solution in ACN; [AN] = 0.1 M and c = 20 mV/s.

Published in: Thin solid films (1997), vol. 310, iss. 1-2, pp. 148-155
Status: Postprint (Author's version)

2. Experimental

The experimental conditions for the electroreduction of AN in ACN and the preparation of the Ni electrodes were previously detailed [2]. The electrodes were carefully polished with abrasive papers of decreasing mesh and finally with an alumina suspension in water (1 μm),so that
substrates with a flatness and roughness suitable to XRR experirnents were made available.
All the samples investigated in this study were prepared by two successive voltannn~etric scans up to the potentiaI at the inhibition peak maximum at a 20 mV/s scanning rate. This voltage was hold for an average of 20 s before either repeating or stopping the experiment. The electrografted films were carefully washed with DMF in order to dissoIve any ungrafted chain and then with ACN. They were finally dried overnight in vacuo at 40°C.
The ellipsometry measurements were carried out with a nulIing-scheme Ll 17 ellipsometer (Gaertner), at a wavelength of 6328 Å (helium-neon laser). A 70° angle of incidence (with respect to the normal to the substrate) was used in the two conjugate zones. At least four measurements were reported for each sample at different locations. Most samples were also analyzed with a 50° angle of incidence.
The XRR measurements were performed with a Siemens DS000 2-circle diffractometer fitted with a sealed copper tube and a graphite secondary monochromator, selecting the Cu K_a radiation (λ= 1.5418 Å). The beam was properly collimated by placing a knife edge a few μm above the sample surface. The data were scaled to unit incident intensity and corrected for background scattering and variation of the illuminated area at very low angles of incidence (below ~ 0.125°, depending on the sample size and position of the knife edge). The data were reported as a function of k_{z0}, the component of the wave vector of the incident photons perpendicular to the interface. Both the ellipsometry and reflectivity measurements were analyzed with a model consisting of homogeneous layers superposed on a flat substrate, using a matrix iterative formalism derived from Fresnel's equations [3–6]. In case of XRR measurements, a parameter σ_{XRR} characteristic of
the roughness of the layers and their mutual interpenetra-tion was also taken into account [7-9]. Actually,O-σ_{XRR} is the standard deviation of a Gaussian whose integral approximates a sigmoidaI variation of the electron density at the interface.
AFM measurements were performed in the contact mode with an Autoprobe CP (Park Scientific Instruments). The stiffness of the cantilevers was ca. 0.2 N/m, and the
scanning rate typically less than 5 *μ/s.* At least 3 regions were analyzed for each sample and the root-mean square (RMS) roughness, σ_{AFM}, was computed by standard image analysis techniques.

3. Results

Fig. 2 shows the XRR data for three PAN films elec-tropolymerized on Ni in DMF. Two of these curves show very weak Kiessig fringes at k_{z0}larger than 0.04Å^{-1}, as a result of interferences between the wave reflected at the nickel/film interface and the wave reflected at the air/film interface. The frequency of these oscillations depends on the film thickness according to the Bragg's law. The slope of the curve at the highest wave vectors mainly depends on the roughness of the smoothest interface. Below the critical wave vector for PAN (0.011Å^{-1}), total reflection should occur. However, due to non-perfect flatness of the sample, this range is strongly, affected by experimental errors; this is why the experimental reflectivity differs from unity at very low angles. Between the critical wave vectors of PAN and nickeI (0.0287 Å^{-1}), the wave is partially absorbed by the PAN film and at the PAN/nickel interface. This effect combined with the interference of the waves reflected at the PAN/Nickel and PAN/air interfaces, gives rise to oscillations in the reflected intensity, whose position depends on the film thickness according to a refraction corrected Bragg's law. Thus, a rapid semi-quantitative analysis of the XRR curves allows preliminary values for the film thickness *(d),* the film roughness (σ_{PAN}). and the electron densities of nickel (ρ_{Ni})and PAN (ρ_{PAN}). The later two values are directly related to the critical wave vectors.
From these preliminary vaIues, a model for the electron density profile perpendicular to the interfaces ($\rho(z)$) is used to fit the experimental data (Fig. 2a and b). The agreement between model and experiment is good except for very small wave vectors, where systematic errors are important. Nevertheless, even in this error-prone range of k_{z0}, the fit satisfactorily approximates the main features of the reflectivity (position and shape of the oscillations) (see inset). The fit parameters are listed in Table 1. The computed electron densities for nickel are in agreement with the theoretical value (2.27 Å^{-3}). The agreement is less ood for PAN (0.38-0.43 Å^{-3}; theoretical value = 0.33 Å^{-3}). This is not surprising, since the accuracy on the electron density of polymers determined by XRR is often low [10]. The roughness at the nickel/PAN interface is small, although the nickel was merely

Published in: Thin solid films (1997), vol. 310, iss. 1-2, pp. 148-155
Status: Postprint (Author's version)

polished.
The roughness at the air/PAN interface has also been measured by AFM (Table 1) and found slightly different from the values estimated by XRR. In case of sample 2, the discrepancy between AFM and XRR measurements is large. This observation results fi'om: (1) The sensitivity of XRR to the (laterally integrated) electron density profile, whereas, AFM probes the surface topography of the sample, Changes in the sample density in the vicinity of the outer surface contribute to σ_{XRR}, but are unobserved by AFM.

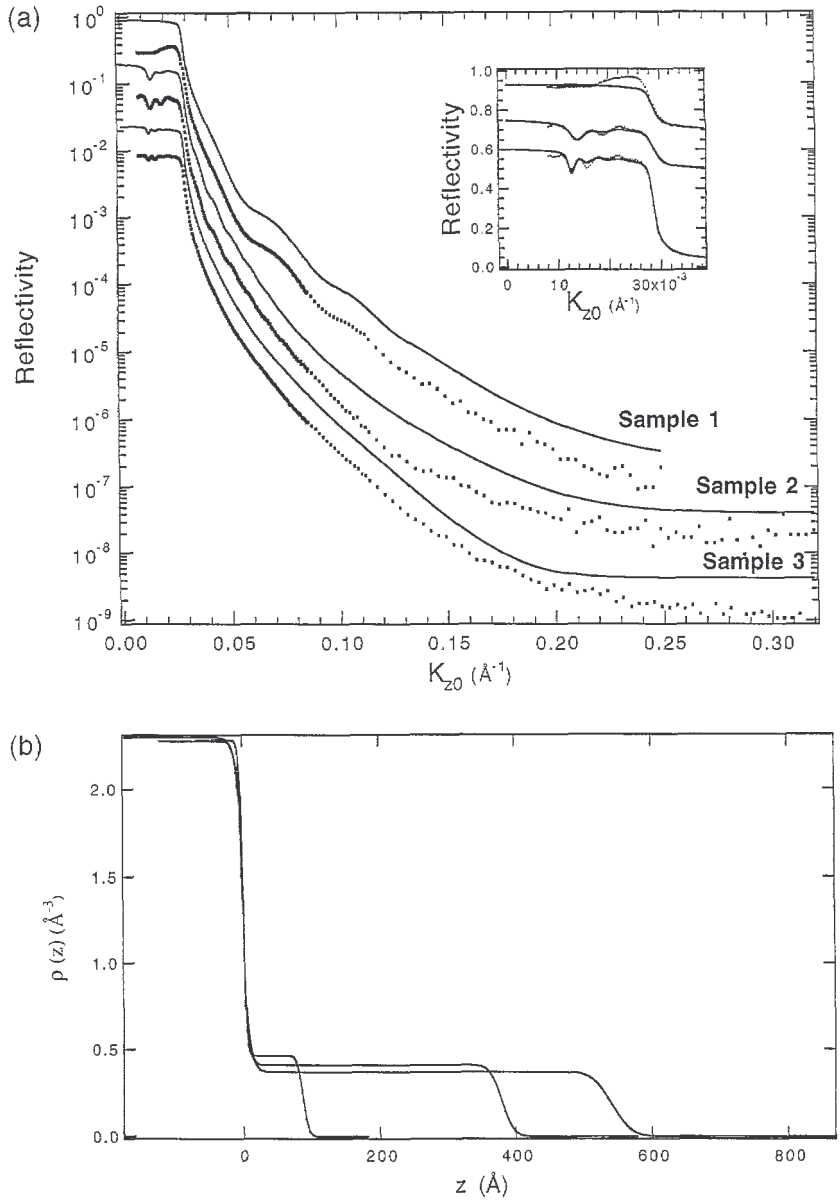

Fig. 2. (a) X-ray refiecfivity data (dots) for samples 1-3 of Table 1, and the best fit (full line), as a function of the component of the wave vector of the incident photon perpendicular to the interfaces (k_{z0}). The reflectivities have been vertically shifted for sake of clarity. (b) Electron density profiles p(: ^{z}) calculated from the fit of the data of (a).

Table 1
Parameters extracted from the fit of the XRR data, and roughnesses determined by AEM, for the samples of this study investigated by XRR

Sample[a]	ρ_{Ni} (Å^{-3})[b]	$\sigma_{Ni,XRR}$ (Å)[c]	ρ_{PAN} (Å^{-3})[d]	$\sigma_{PAN,XRR}$ (Å)[e]	d (Å)[f]	$\sigma_{PAN,AFM}$ (Å)[g]
1	2.24	10	0.38	9	87	5
2	2.25	12	0.43	22	377	6
3	2.25	16	0.42	33	540	21
4	2.21	19	0.42	19	202	29
5	2.27	15	0.43	15	204	25

Published in: Thin solid films (1997), vol. 310, iss. 1-2, pp. 148-155
Status: Postprint (Author's version)

[a]Samples 1 to 3 were prepared in DMF, respectively, with [AN] = 0.1 M, 0.2 M, and 0.3 M. Samples 4 and 5 were synthesized in ACN, respectively with [AN] = 0.5 M and 2 M. For all samples, the deposition technique was voltammetry scans.
[b]ρ_{Ni}: electron density of nickel.
[c]$\sigma_{Ni,XRR}$: roughness of the Ni/PAN interface, as determined by XRR.
[d]ρ_{PAN}: electron density of PAN.
[e]$\sigma_{PAN,XRR}$: roughness of the PAN/air interface, as determined by XRR.
[f]d: thickness of the PAN film.
[g]$\sigma_{PAN,AFM}$: roughness of the PAN/air interface, as determined by AFM.

Table 2
Literature data on refractive index of nickel. $\lambda = 6328$ Å

Authors	Reference	Year	Refractive index of nickel $\lambda = 632$		Conditions
			Real part	Im. part	
S. Roberts	[23]	1959	1.88	3.72	Machined and electro-polished
E. Menzel, J. Gebhart	[24]	1962	2.17	4.17	Solidified drop
D.W. Lynch, R. Rosi, J.H. Weaver	[25]	1971	1.98	3.74	(111) surface at 4 K. Spark cut, polished and etched.
P.B. Johnson, R.W. Christy	[19]	1974	1.99	4.12	Vacuum evaporated and annealed
A.A. Studna	[29]	1975	1.61	3.37	(110) surface, mechanical and optical polish
T. Smith	[18]	1976	2.20	4.16	Mechanical polish, anneal and ion bombardment
F.C. Schouten, E.W. Kalcveld. G.A. Bootsma	[30]	1977	2.23	4.17	Ni(110) spark cut, polished, sputtering, oxygen exposure at room temperature and heating
M.Ph. Stoll, C. Jung	[31]	1979	2.20	4.22	(110) surface, polished by hand and thermal treatment (700 K)
H.F. Hazebroek, W.M. Visscr	[32]	1983	2.245/2.155	4.068/4.248	(111) surface, polished. Anisotropy in the plane of the surface
L.J. Hanekamp, S.J.H. Brader, G.A. Bootsma	[22]	1983	2.27	4.21	(110) surface. Spark erosion, mechanically and electrochemically polished. Cycles of ion bombardment and annealing
C. Calberg et al.	This work	1996	2.11	3.94	Mechanically polished + electro-chemically reduced. Covered with a protective PAN film

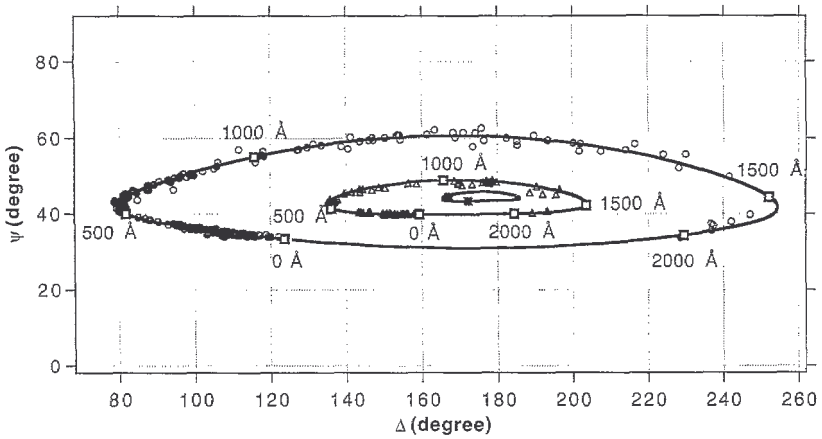

Fig. 3. Dependence of the thickness of PAN films on the ac~,lonitrile concentration in DMF (circles) and ACN (squares). Error bars correspond to the standard error computed on the average of at least five measurements performed on the same sample (the full line is a guide for eyes).

(2) The limited sampling of the AFM technique, compared to the macroscopic surface probed by XRR. (3) The usual dependence of the roughnesses on the length scale, L_σ,, over which the average is performed, due to lateral correlations between asperities [7– 9]. In case of XRR, L_σ corresponds to the coherence length of the photons (which depends on the incident angle in this study), whereas, it corresponds to the size of the scanned area in the AFM technique. A recent paper has examined these differences for magnetic multilayers [11].

A more complete comparison of σ_{AFM} and σ_{XRR} would require measurements of σ_{AFM} at many more locations and for a wide range of magnification powers. This is outside the scope of the present study. The interested reader should consult Refs. [12-14] for further details about this point.
The severe constraints on the sample flatness, and the long time required by the XRR measurements, prompted us to resort to the much faster and less demanding ellip-sometry in order to measure the fihn thickness.

Ellipsome-try has the further advantage to be able to monitor the 'in situ' film growth during polymerization [15]. However, computation of film thicknesses from ellipsometric angles requires the knowledge of the refractive indices, η, of PAN and nickel at the selected wavelength, Inspection of the literature reveals that the index of refraction of nickel (η_{Ni}) is not known with accuracy (Table 2).

Fig. 4 shows the measured ellipsometric angles ψ and Δ for samples prepared under different experimental conditions. At a given incidence angle, the measurements describe a continuous curve in the (ψ, Δ) plane, (ψ, Δ) rotates clockwise along these curves upon increasing film thickness. For non-absorbing films, such as PAN, (ψ, Δ) returns to the 0 Å point after a given period (PAN, 70°; 2677 Å), A model consisting of a homogeneous layer on a flat substrate has been used to fit these data (continuous lines of Fig. 3). The parameters of the model are the film thickness (for each data point, except for 5 samples for which the thickness was known from XRR), the complex refractive index of nickel and the refractive index of PAN (η_{PAN}). Results are η_{PAN} = 1.51 and η_{Ni}r/Ni=2.tl (+0.05) $+j$ 3.94 (_+0.05). The value for PAN is in good agreement with the literature data $(\eta_{PAN}$ = 1.5--1.53 [16]). It is worth noting that the refractive indices of PAN for electric fields parallel and perpendicular to the chain axis are equal within 0.005 [16], thereby, alleviating the need to consider a possible orientation of the chains with respect to the substrate, [1] The value found for nickel ties in the range of the values reported in the literature for λ = 6328 Å (Table 2).

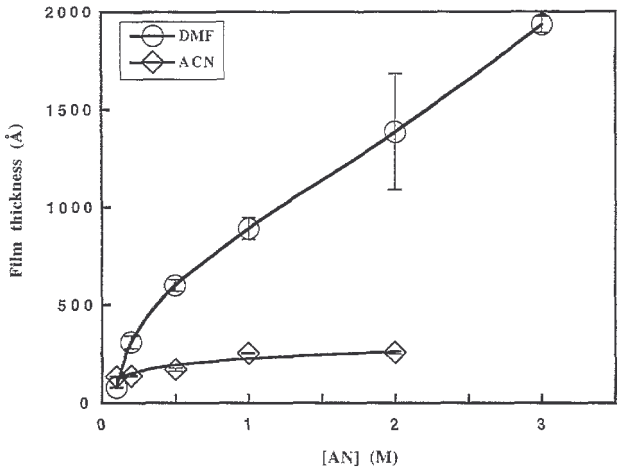

Fig. 4. Measured ellipsometric angles ψ and Δ for samples prepared under different conditions (solvent, acrylonitrile concentration, etc.) and best fit to these data (full lines). Data are distributed in a clockwise manner on the curve as the film thickness is increased. "Squares' indicate the theoretical location in the (ψ, Δ) plane of films of 0. 500, 1000. 1500 and 2000 A thickness. Measurements have been carried out at three different angles (with respect to the sample normal): 70° (circles), 50° (triangles), 30° (stars).

Table 3
Comparison of the thicknesses determined by, XRR and ellipsometry. (Nomenclature as in Table 2)

Sample	Thickness determined by XRR (Å)	Thickness determined by ellipsometry (Å)
1	87	89
2	377	37i
3	540	572
4	202	204
5	204	200

The large scattering of the reported refractive indices for nickel results from differences in the preparation of the surface (polishing, annealing, ion bombardment, etc.), that affects the surface characteristics (roughness, segregation of impurities, etc.) [18-25], or from variations in the aggregation state (single crystals, polycrystalline bulk and film samples, etc.) [20,22]. Particularly important is the possible existence of an oxide layer on the nickel surface, which decreases reflectance and affects the phase shift upon reflection. In this study, the oxide layer is reduced before electropolymerization is started, and it cannot grow up again afterwards since the sites are occupied by the grafted polymer. Furthermore, since the samples have not been annealed and since the po!ished Ni surfaces have a small RMS roughness ($\sigma \approx$ 15 Å) as shown by XRR, our experimental value

[1] Birefringence of PAN affects computed thicknesses by less than 1%.

for η_{Ni} is close to the actual value of bare polycrystalline nickel. This problem has a practical relevance, since some of the values reported in Table 2 can lead to changes as large as 30% in the computed film thickness. The aforementioned Ni value has been used in this study, and has provided a good agreement for thicknesses determined by XRR and ellipsometry (Table 3).
The influence of several polymerization conditions on the PAN film thickness is illustrated in Fig. 3. The thickness strongly depends on both the AN concentration and the solvent nature (DMF or ACN). By contrast, the number of deposition cycles (although limited in this study) and the deposition technique (voltamperometry, chronoam-perometry, and chronopotentiometry) has no decisive influence on the final thickness (Table 4). It is noteworthy that the thickness measured by ellipsometry is essentially independent of the probed area for a given sample (typically within 10%).

Table 4
Effect of tile deposition technique and the number of deposition cycles on the thickness of the electrografted PAN. All samples were synthesized in DMF ([AN] = 0.5) with the same batch of solvent and monomer

Thickness (Å.)	Technique	Number of deposition cycles
1138	Chronoamperometry	2
1139	Chronopotentiometry	2
1018	Voltamperometry	1
1178	Voltamperometry	2

Much larger variations are found when several samples are prepared under the same experimental conditions, resulting from some differences in the electrode surface and the residual water in the solvent. The higher polarity of DMF compared to ACN makes the water elimination more touchy and may account for larger variations in case of samples prepared in DMF rather than in acetonitrile. Finally, it must also be noted that the relative roughnesses (σ_{AFM}/d) of the films prepared in DMF tend to be smaller than for films prepared in aceto-nitrile.

4. Discussion

According to the mechanism proposed for the AN electroreduction, the inhibition peak observed at the lowest cathodic potential is the signature of the grafting reaction. It is indeed at this potential that the electrodeposition of an adherent thin film is observed to passivate the cathode even in a solvent (DMF) for PAN. This situation is in sharp contrast to the case where the electropolymerization occurs at a potential higher than the inhibition peak and in a non-solvent for PAN, such as ACN. Then, a non-adherent film is deposited on the electrode, which is not passivated. In this study, all the films have been electropoly-merized in the potential range of the inhibition peak, and the reported thickness is thus typical of monolayers of PAN grafted chains. Fig. 3 compares the thickness of PAN films electrografted in either DMF or ACN. The results indicate that the film thickness increases with the monomer concentration. This observation is consistent with the radical mechanism reported for the electrografting reaction [2]. It is indeed known that propagation of radical polyaddition depends on monomer concentration, in contrast to termination which only depends on concentration of the growing chains. As a result, the kinetic chain length, and in this case the thickness of the grafted PAN layer, is directly affected by the AN concentration. Data in Fig. 3 are thus an additional although indirect evidence for the radical nature of the species originally grafted onto the cathode and growing away from the metal.
In the particular case where the growing (radical) chains are tethered on a surface, it is not surprising that bimolecular collisions are more probable and that the chain length tends to level off when the AN concentration is high enough. Fig. 3 also clearly shows that the film thickness is strongly dependent on the solvent, being much smaller in ACN compared to DMF. This observation can be rationalized by precipitation of the growing PAN chains in ACN and solvation in DMF. As soon as the PAN chains reach some critical length in ACN, they precipitate on the electrode, which is very detrimental to propagation to the point where termination dominates either by radicaI recombination or disproportionation or by transfer, e.g., to monomer. The maximum thickness of the PAN film in ACN should thus be controlled by the rapid loss of solubility when the chain molecular weight increases. Although this situation does not prevail in DMF, the film thickness also tends to level off, but at a much higher value than in ACN. This observation is thought to be also of a kinetic origin. Indeed, the monomer concentration in the close vicinity of the electrode is controlled by diffusion and can rapidly decrease as polymerization propagates. Accordingly, the propagation rate decreases, in contrast to the rate of chain termination which remains essentially constant and becomes the critical step for the chain length. This qualitative explanation of the solvent effect on the PAN film thickness is supported by AFM observations reported elsewhere [26]. Indeed, films deposited in ACN are more heterogeneous, as a result of chain precipitation, than films prepared in DMF, which appear to be more uniform and regular in surface. These characteristics reflect a rather homogeneous initiation on the electrode surface in DMF, the solvatation of the growing chains during the whole polymerization in this solvent and a higher film thickness. From the experimental dependence of the

thickness of the electrografted PAN film on the AN concentration and solvent, it appears that a large range of thicknesses front 85 to 2000 A can be covered. It is worth noting that when the monomer concentration is decreased, the two reduction peaks, i.e., the inhibition peak moves to the diffusion peak, so that they ultimately overlap at [AN] smaller than 5.10^{-2}-M. Then, no grafting occurs and more and the lower limit of thickness is thus close to 85 A. The upper limit of 2000 Á is imposed by kinetics of the radical polyaddition of AN as previously explained. In agreement with a film thickness controlled by solvent and monomer concentration according to a radical growth mechanism, Table 4 shows that the thickness of PAN films electrodeposited under the same conditions of solvent and AN concentration is essentially independent of the technique used for the initiation, i.e., chronoamperometry, chronopotentiometry and voltam-perometry. An additional deposition cycle has also a very limited effect in agreement with an already efficient passivation at the end of the first scan.
On the assumption that the grafted PAN chains are fully extended, which is not true although acceptable according to Reynaud et al. [27], the average degree of polymerization (DP) for PAN can be approximated to 35 (Mn = 1860) and 820 (Mn = 43,400) for the lower and upper thickness, respectively.
Results of Fig. 4 disagree with Leroy et al. [28], who published thicknesses of several thousands Á in ACN. This discrepancy might however result from the potential at which the electropolymerization has been carried out. Would it occur even early in the potential range of the more cathodic voltammetric peak, then the deposited film should be a mixture of grafted and ungrafted chains precipitated onto the electrode in ACN. Under these conditions, the longer the polymerization time is and the thicker the electrodeposited film. The results reported in this paper clearly show that the thickness of the electrografted PAN chains can be controlled over a decade, i.e., from 85 up to 2000 A, while changing the AN concentration (from 5.10^{-2} M to 3 M) and the ability of the reaction medium to solvate the growing PAN chains.

Acknowledgements

Part of this work was supported by the 'Ministère de la Région Wallonne' as a 'FIRST Research Program' (no. 2585). The authors are also grateful to the 'Services F~d4raux des Affaires Scientifiques, Techniques et Culturelles (PAI Polymères)' for support to CERM. They thank the 'R&D Groupe Cockerill Sambre' for continuous interest and fruitful discussions. Financial support from the Belgian National Fund for Scientific Research (AMJ) and from the "Direction G~n~rale de la Recherche Scientifique de la Communauté Française de Belgique' (convention 94/99-173) (XA) is also gratefully acknowledged.

References

[I] G. Lecayon, Y. Bouizem, C. Le Gressus, C. Reynaud, C. Boiziau, C. Juret, Chem. Phys. Lett. 91 (1982) 506.
[2] M. Mertens, C. Calberg, L. Martinot, R. Jérôme, Adv. Mater. 7 (1995) 807.
[3] J. Lekner, Theory of Reflection of Electromagnetic and Particle Waves, Martinus Nijhoff Publishers, Dordrecht, 1987.
[4] R.M.A. Azzam, N.M. Bashara, Ellipsometry and Polarised Light, Elsevier, Amsterdam, 1987.
[5] L.G. Parratt, Phys. Rev. 95 (1954) 359.
[6] L.G. Parratt, J. Chem. Phys. 53 (1956) 597.
[7] S.K. Sinha, E.B. Sirota, S. Garoff, H.B. Stanley, Phys. Rev. B 38 (1988) 2297.
[8] S.K. Sinha, M.K. Sanyal, S.K. Satija, C.F. Majkzak, D.A. Neumann, H. Homma, S. Szpala, A. Gibaud, H. Morkoc, Phys. B 198 (1994) 72.
[9] L. Névot, P. Croce, Rev. Phys. Appl. 15 (I980) 761.
[10] A.C. Zeppenfeld, S.L. Fiddler, W.K. Ham, B.J. Klopfenstein, C.J. Page, J. Am. Chem. Soc. 116 (1994) 9158.
[11] K. Temst. M.J. Van Bad, B. Wuyts, C. Van Haesendonck, Y. Bruynseraede, D.G. de Groot, N. Koeman, R. Griessen, AppI. Phys. Lett. 67 (1995) 3429.
[12] Z.-H. Cai, K. Huang, P.A. Montano, T.P. Russell, J.M. Bai, G.W. Zajac, J. Chem. Phys. 98 (1993) 2376.
[13] C. Thompson, G. Palasantzas, Y.P. Feng, S.K. Sinha, J. Krim, Phys. Rev. B 49 (1994) 4902.
[14] M. Yanagihara, T. Sasaki, M. Furudate, M. Yamamoto, Opt. Rev. 3 (1996) 65.
[15] Y. Bouizem, F. Chao, M. Costa, A. Tadjeddine, G. Lecayon, J. Electroanal. Chem. Interracial Chem.
[16] J. Brandrup, E.H. Immergut, Polymer Handbook, 3rd edn., Wiley, New York, 1989.
[17] (1984) 101.
[18] T. Smith, J. Opt. Soc. Am. 67 (1977) 48.
[19] P.B. Johnson, R.W, Christy, Phys. Rev. B 9 (1973) 5056.
[20] F.H.P.M. Habraken, O.L,J. Gijzeman, G.A. Bootsma, Surf. Sci. 96 (t980)482.
[21] M. Gadenne, J. Lafait, J. Phys. 47 (1986) 1405.
[22] L,J. Hanekamp, S.J.H. Brader, G.A. Bootsma, Surf. Sci. 135 (I983) 383.
[23] S. Roberts, Phys. Rev. 114 (1959) I04.

[24] E. Menzel, J. Gebhart, Z. Phys. 168 (1962) 392.
[25] D.W. Lynch, R. Rosei, J.H. Weaver, Solid State Commun. 9 (1971) 2195.
[26] M. Mertens, C. Calberg, L. Martinot, R. J~rgme, V. Geskin, R. Lazzaroni, J.L. Brédas, submitted to Macromolecules.
[27] C. Reynaud, C. Boiziau, C. Juret, S. Leroy, J. Perreau, G. Lecayon, Synth. Met. 11 (1985) i59. [28] S. Leroy, C. Boiziau, J. Perreau, C. Reynaud, G. Zalczer, G. Lecayon, C. ke Gressus, J. Mol. Struct.
[28] (1985) 269.
[29] A.A. Studna, Solid State Commun. 16 (1975) 1063.
[30] F.C. Schouten, E.W. Kaleveld, G.A. Bootsma, Surf. Sci. 63 (1977) 460.
[31] M.Ph. Stoll, C. Jung, J. Phys. F 9 (I979) 2491. [32] H.F. Hazebroek, W.M. Visser, J. Phys. E 16 (1983) 654.